https://doi.org/10.1007/s11467-023-1388-x

RESEARCH ARTICLE

A universal non-Hermitian platform for bound state in the continuum enhanced wireless power transfer

Haiyan Zhang[1], Zhiwei Guo[1,†], Yunhui Li[2], Yaping Yang[1], Yuguang Chen[1,‡], Hong Chen[1]

[1]School of Physics Science and Engineering, Tongji University, Shanghai 200092, China

[2]Department of Electrical Engineering, Tongji University, Shanghai 201804, China

Corresponding authors. E-mail: †2014guozhiwei@tongji.edu.cn; ‡ygchen@tongji.edu.cn

Received December 25, 2023; accepted January 16, 2024

Supplementary Information

Note 1. Stability of the BIC-assisted second-order and third-order WPT systems

In the main text, the intrinsic loss is not considered when analyzing the BIC condition for the optimal efficiency of the second-order and third-order WPT systems, for the convenience of analysis, we have made a simple treatment, namely, let $\Gamma_1 = \Gamma_2 = \Gamma = 0$ in the second−order WPT system and $\Gamma_1 = \Gamma_2 = \Gamma_3 = \Gamma = 0$ in the third-order WPT system, and the efficiency reaches its maximum rightly at BIC. However, we find that the condition of achieving efficiency maxima is not consistent with the condition of BIC when the intrinsic loss is not negligible.

Specifically, for the lossy second-order system in Fig. 1(b), that is $\Gamma_1 = \Gamma_2 = \Gamma \neq 0$, when considering the system working at the intrinsic frequency ω_0, we can rewrite Eq. (13) as

$$\eta = \left|\frac{2\sqrt{g_1\gamma_2}\kappa}{\kappa^2+(g_1+\Gamma_1)(\gamma_2+\Gamma_2)}\right|^2. \tag{S1}$$

Moreover, the conditions of efficiency maxima are not the same when different parameters are adjusted, including gain rate, loss rate or coupling strength. In detail, as for the case of tuning the coupling strength of κ, the derivative of the transmission coefficient S_{21} with respect to the coupling strength κ is obtained as

$$\frac{dS_{21}}{d\kappa} = \frac{2\sqrt{g_1\gamma_2}[\kappa^2+(g_1+\Gamma_1)(\gamma_2+\Gamma_2)]-2\kappa 2\kappa\sqrt{g_1\gamma_2}}{\kappa^2+(g_1+\Gamma_1)(\gamma_2+\Gamma_2)}. \tag{S2}$$

Let $\frac{dS_{21}}{d\kappa} = 0$, then we can get the maximum transfer efficiency condition is

$$\kappa^2 = (g_1+\Gamma_1)(\gamma_2+\Gamma_2). \tag{S3}$$

As for the case of tuning the gain rate of g_1, let

$$\frac{dS_{21}}{dg_1} = \frac{2\kappa\sqrt{\frac{\gamma_2}{g_1}}[\kappa^2+(g_1+\Gamma_1)(\gamma_2+\Gamma_2)]-2\kappa\sqrt{g_1\gamma_2}(\gamma_2+\Gamma_2)}{\kappa^2+(g_1+\Gamma_1)(\gamma_2+\Gamma_2)} = 0. \tag{S4}$$

Then we can get the maximum transfer efficiency condition is

$$\kappa^2 = (g_1-\Gamma_1)(\gamma_2+\Gamma_2). \tag{S5}$$

As for the case of tuning the loss rate of γ_2, let

$$\frac{dS_{21}}{d\gamma_2} = \frac{2\kappa\sqrt{\frac{g_1}{\gamma_2}}[\kappa^2+(g_1+\Gamma_1)(\gamma_2+\Gamma_2)]-2\kappa\sqrt{g_1\gamma_2}(g_1+\Gamma_1)}{\kappa^2+(g_1+\Gamma_1)(\gamma_2+\Gamma_2)} = 0. \tag{S6}$$

Then, the maximum efficiency condition is

$$\kappa^2 = (g_1+\Gamma_1)(\gamma_2-\Gamma_2). \tag{S7}$$

Similarly, for the lossy third-order system in Fig. 1(c), that is, $\Gamma_1 = \Gamma_2 = \Gamma_3 = \Gamma \neq 0$, at this time, the transfer efficiency at $\omega = \omega_0$ can be deduced as

$$\eta = |S_{21}|^2 = \left| -\frac{2\sqrt{g_1\gamma_3}\kappa_{12}\kappa_{23}}{g_1\kappa_{23}^2+\gamma_3\kappa_{12}^2+(\kappa_{12}^2+\kappa_{23}^2+g_1\gamma_3)\Gamma+(g_1+\gamma_3)\Gamma^2+\Gamma^3} \right|^2. \tag{S8}$$

Moreover, the conditions of efficiency maxima are not the same when different parameters are adjusted, including gain rate, loss rate or coupling strength. In detail, as for the case of tuning the coupling strength of κ_{23}, the derivative of the transmission coefficient S_{21} with respect to the coupling strength κ_{23} is obtained as

$$\frac{dS_{21}}{d\kappa_{23}} = \frac{2\sqrt{g_1\gamma_3}\kappa_{12}[\kappa_{23}^2(g_1+\Gamma)-(\gamma_3+\Gamma)(\kappa_{12}^2+g_1\Gamma+\Gamma^2)]}{[(\gamma_3+\Gamma)(\kappa_{12}^2+g_1\Gamma+\Gamma^2)+\kappa_{23}^2(g_1+\Gamma)]^2}. \tag{S9}$$

Let $\frac{dS_{21}}{d\kappa_{23}} = 0$, then we can get the maximum transfer efficiency condition is

$$\kappa_{23}^2(g_1+\Gamma) = (\gamma_3+\Gamma)(\kappa_{12}^2+g_1\Gamma+\Gamma^2). \tag{S10}$$

Similarly, as for the case of tuning the gain rate of g_1, let $\frac{dS_{21}}{dg_1} = 0$, then we can get the maximum transfer efficiency condition is

$$\kappa_{23}^2(g_1-\Gamma) = (\gamma_3+\Gamma)(\kappa_{12}^2-g_1\Gamma+\Gamma^2). \tag{S11}$$

As for the case of tuning the loss rate of γ_3, let $\frac{dS_{21}}{d\gamma_3} = 0$, then we can get the maximum transfer efficiency condition is

$$\kappa_{23}^2(g_1+\Gamma) = (\gamma_3-\Gamma)(\kappa_{12}^2+g_1\Gamma+\Gamma^2). \tag{S12}$$

The above three conditions are consistent with the BIC condition of $g_1\kappa_{23}^2 = \gamma_3\kappa_{12}^2$ when the intrinsic loss is negligible, that is, $\Gamma_1 = \Gamma_2 = \Gamma_3 = \Gamma \neq 0$. However, compared with other physical quantities (gain rate, loss rate, coupling strength), this difference is negligible when the intrinsic loss is small enough.

Note 2. More details about the experiment

In this work, all coils are fabricated from Litz wires with a width of 1.92 mm (0.1 mm×200 strands) and attached tightly to the poly (methyl methacrylate) (PMMA) hollow circular cylinder with an outer radius of R = 15 cm. The resonant (non-resonant) coils are wound with 16 (3) turns, and all coils are arranged on a wooden rod and able to slide coaxially. All relevant electrical parameters are measured by using the precision LCR digital bridge (AT2818, Applient) as follows: $L \approx 147$ μH, $C \approx 1.50$ nF, therefore, the resonant frequency of each resonant coil is adjusted to 338.9 kHz. Besides, the capacitance is made up of a lumped−metallized polyester film capacitor (the withstand voltage more than 2000V). The information provided by the WPT system is then read by a $-R$ and R terms connected to Port 1 and Port 2 of the vector network analyzer (Keysight E5071C 9 kHz−4.5 GHz, the source impedance is 50 Ω), respectively, for measuring the reflection (S_{11}) and transmission (S_{21}) spectrums, where $\eta = |S_{21}|^2$ represents the power transfer efficiency. The schematic diagram and experimental sample diagram of the second−order WPT system are shown in Fig. S1, which consists of two resonant (transmitter and receiver) coils and two non−resonant (source and load) coils.

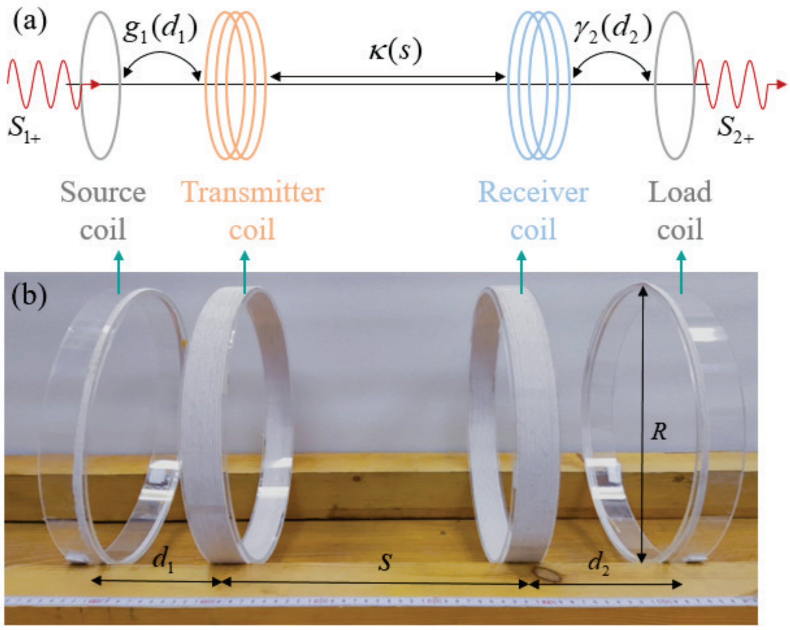

Fig. S1 Second-order non-Hermitian WPT systems. **(a)** Second-order WPT system consisting of two resonant (transmitter and receiver) coils and two non-resonant (source and load) coils. **(b)** Experimental sample diagram corresponding to (a).

Note 3. Details of fitted model parameters

Here, measured coupling rates, as well as fitted results, versus coupling distances are presented in Fig. S2, including $g_1(d_1)$, $\gamma_3(d_2)$, $\kappa_{12}(s_{12})$ and $\kappa_{23}(s_{23})$. Firstly, to characterize the gain rate $g_1(d_1)$, as shown in Fig. S2(a), the transmitter coil with resonance mode $a_0 = A_0 e^{-i\omega t}$ excited by the source coil is analyzed, and the dynamic equation based on coupled-mode theory [1, 2] can be written as

$$\frac{da_0}{dt} = (-i\omega_0 - g_1 - \Gamma_1)a_0 + \sqrt{2g_1}S_{1+}e^{-i\omega t}, \tag{S13}$$

where ω_0, Γ_1 and S_{1+} are the resonance frequency, intrinsic loss, and amplitude of the input wave at Port 1, respectively. g_1 denotes the gain rate, which is determined by the distance between the source coil and the transmitter coil, and the reflection coefficient of Port 1 is

$$S_{11} = \left|\frac{-S_{1+}+\sqrt{2g_1}a_0}{S_{1+}}\right| = -1 + \frac{2ig_1}{(\omega-\omega_0)+i(g_1+\Gamma_1)}. \tag{S14}$$

At the resonance frequency of $\omega = \omega_0$, we can get

$$|S_{11}|_{\omega=\omega_0} = \frac{g_1-\Gamma_1}{g_1+\Gamma_1}. \tag{S15}$$

The half–height width ($\Delta\omega$) of the reflection spectrum corresponds to

$$\Delta\omega = 2(g_1 + \Gamma_1). \tag{S16}$$

By combining Eqs. (S15) and (S16), g_1 and Γ_1 can be obtained, then data fitting is implemented to obtain the relationship between g_1 and d_1, as presented in Fig. S2(b). In addition, considering fitting the relationship between coupling strength and transfer distance, a sufficiently small coil with a negligible gain rate is used to excite two resonance-coupled coils, as presented in Fig. S2(c). In this case, the eigenvalues of the equivalent

Hamiltonian of the system are approximately $\omega_0 - \kappa_{12}$ and $\omega_0 + \kappa_{12}$, that is, the difference in frequency between the two peaks of the reflection spectrum is $2\kappa_{12}$. Similarly, data fitting is implemented to obtain the relationship between κ_{12} and s_{12}, as presented in Fig. S2(d).

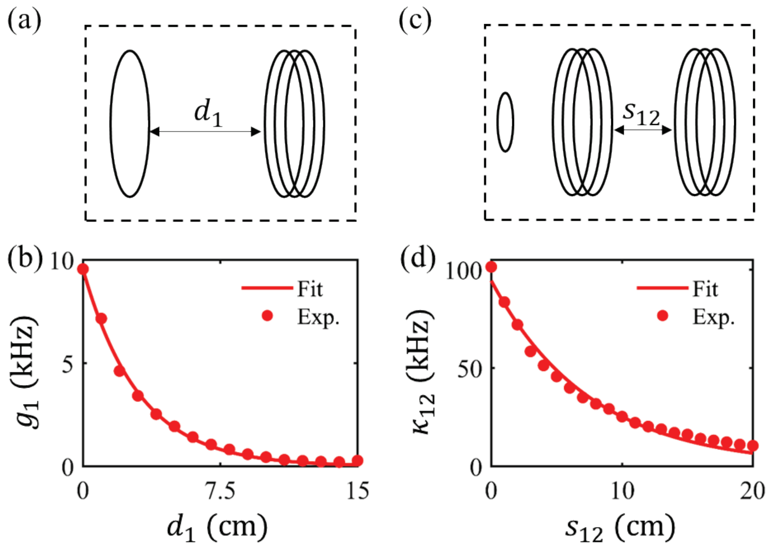

Fig. S2 Coupling rates as a function of separation distance corresponding to the coils in Fig. 4(b). **(a)** The schematic diagram for characterizing gain and loss rates and **(b)** coupling rates between the source (load) coil and transmitter (receiver) coil as a function of separation distance. The fitting result is $g_1 = 9.55e^{-0.3267d_1}$ kHz and $\gamma_3 = 9.55e^{-0.3267d_2}$ kHz. **(c)** The Schematic diagram for characterizing the coupling strengths between adjacent resonant coils and **(d)** coupling rates between transmitter (relay) coil and relay (receiver) coil as a function of transfer distance. The fitting result is $\kappa_{12} = 94.43e^{-0.1318s_{12}}$ kHz and $\kappa_{23} = 94.43e^{-0.1318s_{23}}$ kHz.

Note 4. BIC-assisted multi-load charging with high efficiency

Thanks for the reviewer's concerns. We use a fourth-order WPT system constructed with dual load terminals as an example to discuss wireless power transfer (WPT) systems with multiple loads based on BIC mechanism. As shown in Fig. S1, the pure real mode known as BIC can always be implemented in the case of multi-load charging, which can be used to achieve fixed frequency high-efficiency WPT.

A characteristic equation can be obtained to analyze the eigenvalues of the dual load WPT system and the fourth-order non-Hermitian system with negligible intrinsic loss is described by

$$H\begin{pmatrix} a_1 \\ a_2 \\ a_3 \\ a_4 \end{pmatrix} = \omega \begin{pmatrix} a_1 \\ a_2 \\ a_3 \\ a_4 \end{pmatrix}. \tag{S17}$$

And the effective Hamiltonian H can be expressed as

$$H = \begin{bmatrix} \omega_0 + i\gamma_1 & \kappa_{12} & 0 & 0 \\ \kappa_{12} & \omega_0 & \kappa_{23} & \kappa_{24} \\ 0 & \kappa_{23} & \omega_0 - i\gamma_2 & 0 \\ 0 & \kappa_{24} & 0 & \omega_0 - i\gamma_3 \end{bmatrix}. \tag{S18}$$

The eigenvalues of H of the fourth-order system can be analyzed. The real and imaginary parts of the eigenfrequencies of the fourth-order WPT system versus the loss rate γ_3 are presented in Fig. S3(b) and Fig. S3(c). It is obvious that the BIC mode can still be found by adjusting appropriate parameters.

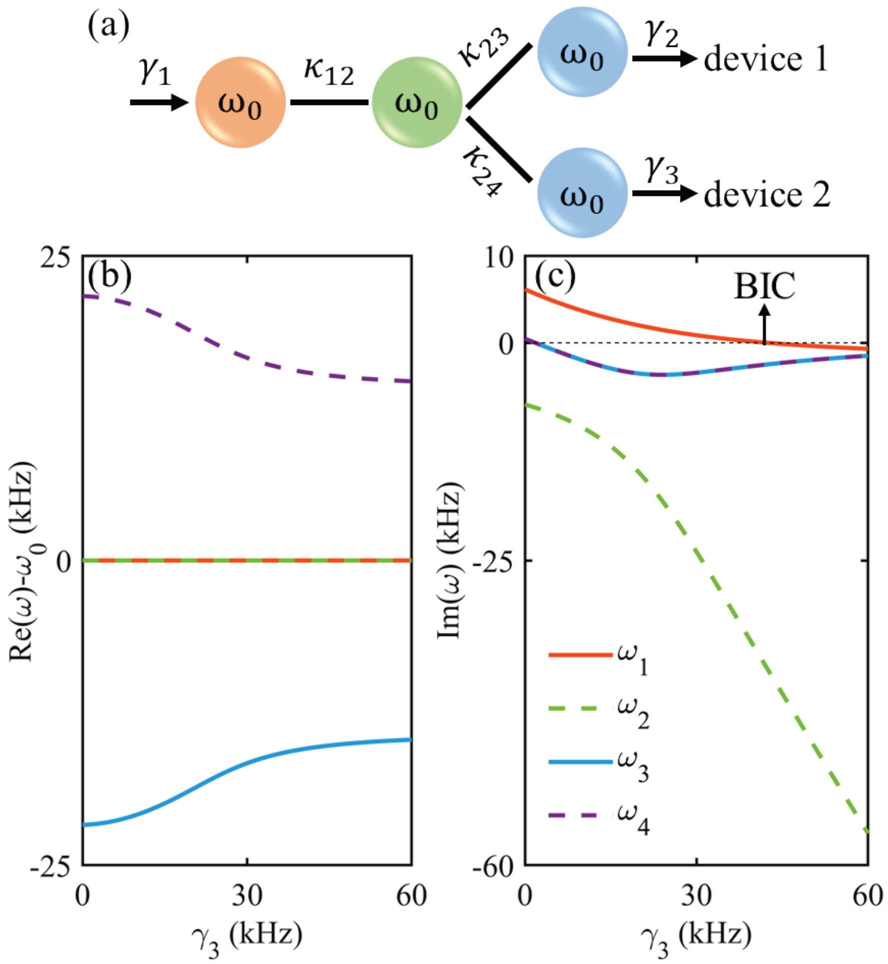

Fig. S3 A multi-load wireless power transfer scheme based on BIC mechanism. **(a)** A fourth-order WPT system with dual loads. Evolution of the **(b)** real part and **(c)** imaginary part of the eigenfrequencies in the fourth-order WPT system with $\gamma_1 = 9.55$ kHz, $\gamma_2 = 9.55$ kHz, $\kappa_{12} = 13.1$ kHz, $\kappa_{23} = 11$ kHz, and $\kappa_{24} = 15$ kHz.

References

1. S. Fan and W. Suh, Temporal coupled-mode theory for the Fano resonance in optical resonators, *J. Opt. Soc. Am. A* **20**, 569 (2003)

2. C. Zeng, et al., Efficient and stable wireless power transfer based on the non-Hermitian physics. *Chinese Phys. B* **31**, 010307 (2022)